JOURNAL OF CATALYSIS 10, 391–400 (1968)

Studies on Pore Systems in Catalysts

XIV. Calculation of the Cumulative Distribution Functions for Slit-Shaped Pores from the Desorption Branch of a Nitrogen Sorption Isotherm

J. C. P. BROEKHOFF AND J. H. DE BOER

From the Department of Chemical Technology, Technological University of Delft, The Netherlands

Received January 15, 1968

The influence of adsorption on capillary evaporation of nitrogen from slit-shaped pores is discussed quantitatively. Thermodynamic reasoning results in a correction to the classical Kelvin equation, similar to that discussed by Derjaguin. The connection between contact angle and capillary evaporation is discussed. It is shown that, except for very wide pores, liquids exhibiting contact angles with the solid adsorbent surface are not suitable for pore distribution analysis from vapor sorption data. The application of the corrected Kelvin equation to the calculation of pore-size distribution functions from nitrogen sorption isotherms is discussed. Examples show the proposed method to lead to satisfactory results in practice.

1. INTRODUCTION

In the preceding parts, IX–XIII, of this series (*1–5*), we have discussed the calculation of cumulative distribution functions from the adsorption branch and the desorption branch, respectively, for cylindrical pores and spheroidal cavities. It was shown there that the influence of adsorption on the equilibria governing capillary evaporation and capillary condensation necessitated the application of certain corrections to the classical Kelvin equation.

In many cases the shape of the hysteresis loop of the vapor sorption isotherm and the shape of the t plot of the adsorption branch indicate the presence of pores which may be approximated by cylinders or spheroidal cavities. In certain instances, however, the B-type hysteresis loop combines with a linear t plot up to high relative pressures. This may be an indication of either ink-bottle pores with rather wide bodies or of slit-shaped pores whose diameters exceed twice the thickness of the adsorbed layer at the highest relative pressure of the linear part of the t plot. When the pores are narrower, downward deviations in the t plot indicate the presence of slit-shaped pores, which become blocked by the adsorbed layer. There are indications that pores of such small diameters do not give rise to hysteresis phenomena during vapor sorption, so probably the concepts of capillarity break down for these narrower pores.

For wider pores, we may analyze the desorption branch of the isotherm for slit-shaped pores if proper corrections are made to the Kelvin equation in order to take into account adsorption in a proper way. This problem was treated before in some detail by Derjaguin (*6*), who derived a corrected Kelvin equation. To our knowledge the equation of Derjaguin has not been used systematically for the analysis of sorption isotherms. The t curve of multimolecular nitrogen sorption on oxidic surfaces (*7*) enables us to make the proper corrections to the Kelvin equation. Following the lines of reasoning given in the earlier parts of this series (*1–5*), we shall derive, in the present paper, an equation for the capillary evaporation which is similar to that derived by Derjaguin but which is more appropriate for use in the micropore region.

The results of cumulative calculations may help to distinguish between ink-bottle pores with wide bodies and slit-shaped pores. In the first case a calculation along the desorption branch of the cumulative surface area for the model of slit-shaped pores will give rise to results that are high in comparison with the surface area as determined from the t plot of the adsorption branch (*8*). Care must be taken to account for the presence of submicropores, however.

2. Thermodynamic Treatment of Evaporation from Slit-Shaped Pores

Generally, it is assumed that, at a certain relative pressure, t_a, the thickness of the adsorbed layer in slit-shaped pores is independent of the pore diameter. This may be erroneous for very narrow pores, but we will assume this to be correct for pores wide enough to exhibit capillary evaporation and hysteresis phenomena.

Thus, contrary to the case of cylindrical pores (*1, 2*), the thickness of the adsorbed layer at each relative pressures is determined solely by the standard adsorption isotherm, which may be written conveniently as

$$RT \ln(p_0/p) = F(t) \qquad (1)$$

For an ideal vapor phase in equilibrium with the adsorbed layer $RT \ln(p_0/p)$ is equal to the difference in thermodynamic potential of the bulk liquid and the adsorbed phase of thickness t at the same temperature. Capillary evaporation from a slit-shaped pore is determined by the equilibrium condition that evaporation of dN moles of condensed phase at constant temperature and pressure does not result in a change in free enthalpy, which in Part IX was shown to be equivalent to the requirement that

$$\gamma \, dA = \Delta\mu \, dN \qquad (2)$$

where γ is the surface tension of the liquid–vapor interface, dA is the change in free surface area of that interface, and $\Delta\mu$ is the difference in thermodynamic potential between the adsorbed phase and the gas phase. Equation (2) has been used before, e.g., by Kiselev (*9*) and by Brunauer (*10*), but in general $\Delta\mu$ is identified with $RT \ln(p_0/p)$, in which case the classical Kelvin equation results. This identification, however, is not permitted, as, on account of adsorption, the thermodynamic potential of the condensed phase in the pore differs from that of the liquid by an amount which depends on the distance to the pore walls, and according to (1) may be expressed as

$$\mu_a = \mu_L - F(t).$$

As a consequence, Eq. (2) may be written as

$$\gamma \, dA = [RT \ln(p_0/p) - F(t)] \, dN \qquad (3)$$

Relation (3) may be used in two, distinct, ways to obtain the corrections to the Kelvin equation for slit-shaped pores.

A. The shape of the meniscus.

Applications of (3) to each point of the meniscus present in a slit-shaped pore filled with condensed phase leads to the equilibrium shape of the meniscus as well as to the conditions of stability. The treatment is completely analogous to that of part XII. In Fig. 1(a) the shape of the meniscus is sketched. A section through the meniscus by a plane perpendicular to the solid surface walls and to the edge of the pores is shown in Fig. 1(b). In a certain point of the meniscus, P, the angle between a tangent to the meniscus and the x-axis of Fig. 1(b), is denoted by a. The curvature of the meniscus at the point P is equal to

$$1/R = d \sin(a)/dx \qquad (4)$$

According to elementary theory of capillarity, in the point P, dA is related to dN by (*11*)

$$dA/dN = V_m/R \qquad (5)$$

where V_m is the molar volume.

Substitution of (4) and (5) into (3) results in the differential equation for the meniscus

$$\frac{1}{R} = \frac{d \sin(a)}{dx} = \frac{1}{(\gamma V_m)} \left[RT \ln\left(\frac{p_0}{p}\right) - F(t) \right] \qquad (6)$$

This equation shows the curvature of the meniscus to be zero for $t = t_a$, viz., at the point of contact between the meniscus and the adsorbed layer.

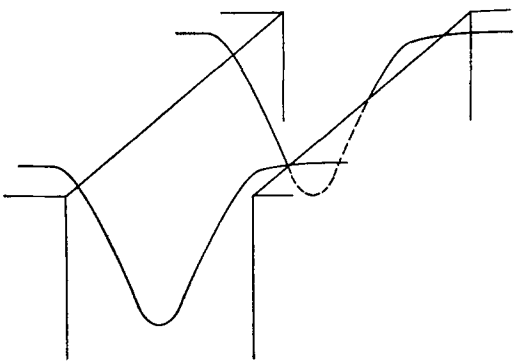

FIG. 1(a). The shape of the meniscus at the edge of a slit-shaped pore.

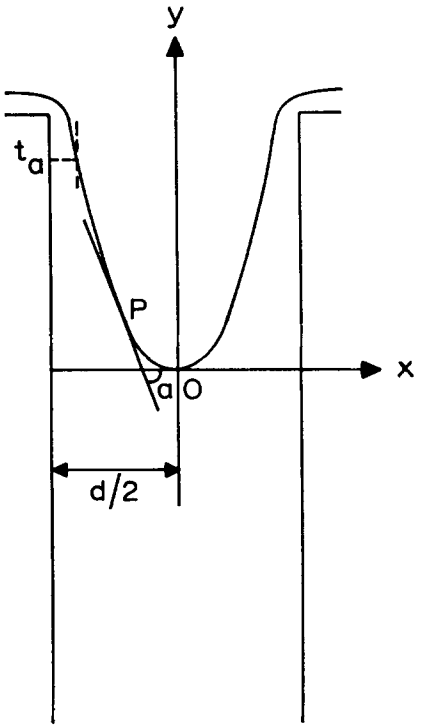

FIG. 1(b). Section through the meniscus

According to Fig. 1(b), x is equal to t-$(d/2)$. Integration of (6), and making use of the obvious boundary condition $\sin(a) = 0$ for $t = d/2$, results in the following relation for the slope of the meniscus:

$$\sin(a) = \frac{1}{(\gamma V_m)}\left[RT \ln\left(\frac{p_0}{p}\right)\left(t - \frac{d}{2}\right) + \int_t^{d/2} F(t)\, dt\right] \quad (7)$$

The complete shape of the meniscus may be obtained from (7), by the substitution

$$dy/dx = \tan(a) = \sin(a)/\,[1 - \cos^2(a)]^{1/2}$$

and integration. This is only possible in very simple cases, e.g., when $F(t)$ is identical to zero, the classical approximation. In this case, $\sin(a)$ is equal to

$$[1/(\gamma V_m)] \times RT \ln(p_0/p)[t - (d/2)]$$

Denoting

$$\gamma V_m/[RT \ln(p_0/p)]$$

by R_k, it is easily shown that the shape of the meniscus is determined by

$$y = R_k - \left[R_k^2 - \left(\frac{d}{2} - t\right)^2\right]^{1/2}$$

which is the equation of a circle with radius R_k. For a stable meniscus to exist, it is clearly necessary that R_k is larger than $(d/2) - t_a$, so the evaporation condition may be written as

$$\frac{d}{2} - t_a = \frac{\gamma V_m}{RT \ln(p_0/p)} \quad (8)$$

which, of course, is the classical Kelvin equation.

For the evaporation of nitrogen from pores in oxidic adsorbents $F(t)$ evidently is not identical to zero and direct analytical integration is impossible, although a numerical solution may be found. The condition of stability, however, may again be found from the consideration that for a stable meniscus the absolute value of $\sin(a)$ as given from Eq. (9) must be less than or equal to 1 for t larger than t_a. The behavior of the shape of the meniscus as a function of pressure exactly ressembles that discussed in Part XII (4) for cylindrical pores. At the evaporation pressure p_D the meniscus is extended infinitely below the point of the contact with the adsorbed layer and at the point of contact the meniscus just touches the adsorbed layer, which means that $\sin(a) = -1$ for $t = t_a$. It immediately follows from (7) that the evaporation pressure $p = p_D$ is determined by the relation

$$\frac{d}{2} - t_a = \frac{\gamma V_m}{TR \ln(p_0/p_D)} + \int_{t_a}^{d/2} \frac{F(t)\, dt}{RT \ln(p_0/p_D)} \tag{9}$$

Equation (9) closely resembles the equation of Derjaguin in a somewhat different formulation and with a different limit of integration.

B. Overall stability condition.

The other way of deriving this equation is more consistent with the treatment of cylindrical pores as discussed in Part IX of this series (*1*). Upon completely filling and emptying the pore by letting the adsorbed layer change in thickness at constant temperature and gas pressure from t_a to $d/2$, the change in interface area is S, the surface of the pore walls. Integration of (3) directly leads to

$$\gamma S = \int_{t_a}^{d/2} \left[RT \ln\left(\frac{p_0}{p_D}\right) - F(t) \right] S \frac{dt}{V_m}$$

viz.,

$$\gamma V_m = RT \ln\left(\frac{p_0}{p_D}\right)\left(\frac{d}{2} - t_a\right) - \int_{t_a}^{d/2} F(t)\, dt \tag{10}$$

For each value of d, this relation is only satisfied at one unique relative pressure p_D/p_0. Only at this pressure is pore filling and pore emptying not accompanied by a change in the free enthalpy of the system. Below this pressure no stable meniscus may exist as pore emptying results in a decrease in free enthalpy of the system. Above this pressure pore emptying results in an increase in free enthalpy of the system so it does not occur. Relation (9) may be immediately rearranged to (10), so both are equivalent. The treatment of Section A has the advantage of leading to an insight into the shape of the meniscus and the process of capillary evaporation.

3. The Role of Contact Angle

In the case of partly wetting liquids some authors prefer to include into the Kelvin equation the contact angle between the liquid and the solid. In the present

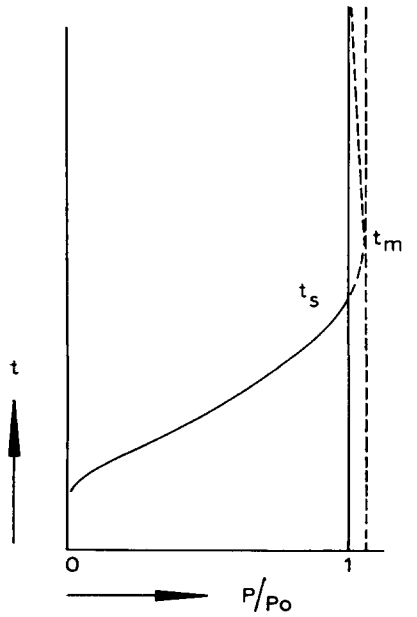

FIG. 2. Possible shape of the adsorption isotherm for the case of contact angle. Hatched part of the isotherm corresponds to metastable states.

treatment the angle between the meniscus and the x-axis (a), which is complementary to the contact angle, is seen to be a function of pressure as well as of pore diameter. At the pressure p_D the contact angle in our treatment is always zero. This contact angle, however, is not the same contact angle as the macroscopic contact angle. If we accept the continuity between the adsorbed phase and the liquid phase in contact with the solid, the basis of the present treatment of capillarity, then the contact angle of capillarity is no independent concept but a property of adsorption when the number of layers adsorbed at the solid surface at saturation is finite. In fact it may be shown that the contact angle of capillarity is a macroscopical concept, which only has significance for a solid in contact with a slab of liquid of infinite thickness. A detailed discussion of this subject is beyond the scope of the present paper, but will be published elsewhere.

If the adsorption isotherm exhibits a finite thickness of the adsorbed layer at $p/p_0 = 1$, denoted by t_s, then the adsorption isotherm corresponding to larger thicknesses corresponds to a metastable supersaturation

branch. However, for very large thicknesses of the adsorbed layer the properties of the adsorbed layer again will tend to those of the bulk liquid. Schematically, the adsorption isotherm may be presented as shown in Fig. 2 (*12*). The adsorption isotherm may be described by a relation of the type of (1), but it is to be realized that for $t > t_s$, $F(t)$ is negative, and generally no empirical representation for $F(t)$ may be found from experimental adsorption determinations.

In principle Eq. (9) remains equally valid, although quantitative evaluation is only possible when $d/2 < t_s$. An exception may be made for very wide pores. To demonstrate this we may write (9) in the form

$$\frac{d}{2} - t_a = \frac{\gamma V_m}{RT \ln(p_0/p_D)} + \frac{\int_{t_a}^{t_s} F(t)\,dt}{RT \ln(p_0/p_D)} + \frac{\int_{t_s}^{d/2} F(t)\,dt}{RT \ln(p_0/p_D)} \quad (11)$$

Realizing that the significance of $F(t)$ is that it is equal to $\mu_L - \mu_a$, we may show by application of the Gibbs adsorption theorem (*13*) that when $d/2$ approximates infinity,

$$\lim_{d/2 \to \infty} \int_{t_s}^{d/2} F(t)\,dt = \gamma V_m[\cos(\varphi) - 1] \quad (12)$$

where φ is the contact angle of capillary. Substitution of (12) into (11) yields the relation

$$\frac{d}{2} - t_a = \frac{\gamma V_m \cos(\varphi)}{RT \ln(p_0/p_D)} + \frac{\int_{t_s}^{t_a} F(t)\,dt}{RT \ln(p_0/p_D)} \quad (14)$$

only valid for very large d, where for p_D/p_0, t_a already will be close to t_s and the correction term at the right side of (14) will be relatively small. It thus is shown that incorporation of the contact angle of capillarity into the Kelvin equation is only admitted for very wide pores. For smaller pores it leads to erroneous results.

One important conclusion that may be drawn from the discussion presented in this section is that such vapors which correspond to liquids which only partially wet the solid adsorbent, should not be used for the analysis of pore sizes from the desorption branch of the isotherms. There are no indications that there is a contact angle between liquid nitrogen and the oxides used as basis for the t curve of multimolecular adsorption: the asymptotic behavior of the sorption isotherms used for the determination of the t curve (*7*) points to complete wetting.

4. Numerical Evaluation of Eq. (9) for Nitrogen at Its Normal Boiling Point

Upon substituting the empirically found relations for the t curve (*2*)

$$\frac{F(t)}{2.303RT} = \frac{13.99}{t^2} - 0.034 \text{ for } t \text{ less } 10 \text{ Å}$$

$$\frac{F(t)}{2.303RT} = \frac{16.11}{t^2} - 0.1682 \exp(-0.1137t) \text{ for } t \text{ greater } 6 \text{ Å}$$

into (9) and integrating, we find for $\gamma = 8.72$ dynes/cm and $V_m = 34.68$ cm³/mole, the following desorption relations:

$$\frac{d}{2} - t_a = \frac{2.02^5 + 13.99(1/t_a - 2/d) - 0.034(d/2 - t_a)}{\log(p_0 p_D)} \quad (15a)$$

and

$$\frac{d}{2} - t_a = \frac{2.02^5 + 16.11(1/t_a - 2d) + 1.483[\exp(-0.5685d) - \exp(-0.1137t_a)]}{\log(p_0 p_D)} \quad (15b)$$

respectively.

The relative pressure regions of the validity of (15a) and (15b), respectively, overlap. In general we may say that (15b) is valid above 0.45 relative pressure, whereas (15a) is a better approximation for more narrow slits. As in the treatment of cylindrical pores (4), it again is assumed that the influence of opposing walls on the relations for $F(t)$ is negligible. This means a nonvalidity of Eq. (15) for very small pores. For these pores the concepts of capillarity break down anyhow, but the significance of Eq. (15) for relative pressures lower

TABLE 1
RELATIVE PRESSURES AT WHICH COMPLETE CAPILLARY EVAPORATION TAKES PLACE, WITH THE CORRESPONDING PORE DIAMETERS (IN Å), IN SLIT-SHAPED PORES

p/p_0	Pore diameter as calculated from (9) (Å)	Pore diameter as calculated from the classical Kelvin equation (Å)
0.9975	4195	3979
0.9925	1504	1383
0.9875	944.1	846.7
0.9825	696.4	612.8
0.9775	555.2	480.5
0.9725	463.2	395.3
0.9675	398.3	336.0
0.9625	349.8	292.6
0.9575	312.3	259.5
0.9525	282.3	233.4
0.9475	257.8	212.4
0.9425	237.4	195.0
0.9375	220.1	180.4
0.9325	205.3	167.9
0.9275	192.4	157.1
0.9225	181.1	147.8
0.9175	171.1	139.5
0.9125	162.2	132.2
0.9075	154.3	125.6
0.9025	147.1	120.0
0.89	131.8	107.4
0.87	113.4	92.30
0.85	99.60	81.12
0.83	88.97	72.47
0.81	80.50	65.48
0.79	73.58	59.79
0.77	67.82	55.13
0.75	62.94	51.15
0.73	58.74	47.71
0.71	55.09	44.71
0.69	51.88	42.04
0.67	49.04	39.67
0.65	46.49	37.54
0.63	44.19	35.61
0.61	42.10	33.85
0.59	40.20	32.24
0.55	36.82	29.39
0.53	35.32	28.12
0.51	33.92	26.93
0.49	32.61	25.82
0.47	31.37	24.78
0.45	30.21	23.79
0.43	29.11	22.86
0.41	28.06	21.98
0.39	6.922	21.13
0.37	25.98	20.33
0.35	25.08	19.56
0.33	24.20	18.82
0.31	23.35	18.11
0.29	22.52	17.42
0.27	21.71	16.75
0.25	20.91	16.10
0.23	20.13	15.46
0.21	19.36	14.84
0.19	18.59	14.21
0.17	17.82	13.60
0.15	17.04	12.99
0.13	16.25	12.36
0.11	15.44	11.73

than, say, 0.40 is uncertain. The influence of the opposing walls itself will lead to even larger pore diameters than those predicted from Eq. (15).

In Table 1 solutions of Eq. (15) for a number of relative pressures are given, together with the diameters predicted by the classical Kelvin equation. The influence of adsorption is seen to result in a substantial increase in predicted pore diameter.

5. CALCULATIONS OF PORE DISTRIBUTIONS

The calculation of pore distributions for slit-shaped pores is far less complicated in practice than that for cylindrical pores (*2*, *4*). Owing to the absence of curvature of the adsorbed layer, the method of Steggerga (*14*) and of Innes (*15*) may be used without modification except for the replacement of Kelvin radii by the solutions of Eq. (15). Again the desorption branch of the isotherm is divided into a number of relative pressure regions, corresponding to a decrease of volume sorbed by the solid (expressed in ml of condensed phase). Over the kth relative pressure region, this decrease is denoted by dV_k^0, the diameter of the pores emptying at the mean relative pressure of the region by d_k, the pore volume of this group of pores by V_k, the corresponding surface area by S_k, the thickness of the adsorbed layer at the high relative

pressure side by t_{k-1} and at the low relative pressure side by t_k. Pore volume and pore surface area may then be calculated from

$$V_k = \frac{d_k}{(d_k - 2t_k)} \left[dV_k^e - (t_{k-1} - t_k) \sum_{i=1}^{k-1} S_i \right] \quad (16)$$

$$S_k = 2V_k/d_k \quad (17)$$

The actual distribution calculation, which is started at saturation, hence at $p/p_0 = 1$, must not be extended downwards further than the closing point of the hysteresis loop. Apart from the uncertainty in the validity of Eq. (9) in the region where hysteresis is no longer observed, *a further extension downwards introduces an error in the value found for S_{cum} from the distribution calculation which is purely mathematical in character.* In the region where no hysteresis is observed, values for dV_k^e from the experimental isotherm are in general small and the influence of the correction term

$$(t_{k-1} - t_k) \sum_{i=1}^{k-1} S_i$$

in each step of the calculation is quite large. The difference between the two terms between the brackets of Eq. (16) is interpreted mathematically as pore volume from pores emptying by capillary evaporation, and apparently such pore volume is found until the value for S_{cum}, the results of the summation series at the right side of the correction term, is equal to the surface area as calculated from the slope of the t plot. Thus, if in the progress of the calculations this cumulative surface area is *not* equal to the total surface area at the closing point of the hysteresis loop, a further extension downwards of the cumulative calculation in many cases leads to a perfect agreement between both quantities even when the t plot indicates the presence of quite narrow slits in the submicropore region where Eq. (9) certainly is not valid. Of course such an agreement has no physical significance whatever. At a relative pressure of 0.4, where no hysteresis is observed anymore with nitrogen as an adsorbate, the theoretical width of the slits is about 28 Å, so we may assume the cumulative surface area at the closing point of the hysteresis loop to be the surface area present in pores wider than 28 Å. In Part VII of this series (*16*) it was shown that for slit-shaped pores the slope of the t plot of the adsorption branch at each relative pressure is a measure of the surface area present in pores wider than twice the thickness of the adsorbed layer at this relative pressure. Thus, the surface area present in pores wider than 28 Å will be given by the slope of the t plot at a relative pressure of approximately 0.88. Unfortunately, there still is some ambiguity with respect to the t value at such high relative pressures (*17*), which, although of little influence on the results of the calculation of pore diameters from Eq. (15b), has a large influence on the determination of the exact slope of the t plot at relative pressures exceeding 0.75 to 0.8. The slope of the t plot at this last relative pressure is a measure of surface area present in pores wider than 20 Å. In this paper it is recommended to compare the cumulative surface area at the closing point of the hysteresis loop to the surface area from the t plot at the highest pressure used, viz., about 0.8. This procedure should lead to physically significant results, and it may be expected that agreement between both quantities is an indication of the soundness of the model of slit-shaped pores. For slits, this test of the pore model is the more important as the possibility of comparing the results from the desorption branch and from the adsorption branch, as in the case of open cylinders (*5*), is absent.

6. Examples of Application

As illustrations of the results of the method proposed in the present paper, we chose some isotherms exhibiting a B-type hysteresis loop, as published by Lippens (*18*) and by van Doorn (*19*). According to Lippens and de Boer, during the dehydration of well-crystallized boehmite, slit-shaped pores are generated, initially together with pores in the submicropore region. According to van Doorn and de Boer, graphitic oxide consists of laminae, with slit-shaped pores in between. These samples seem to be

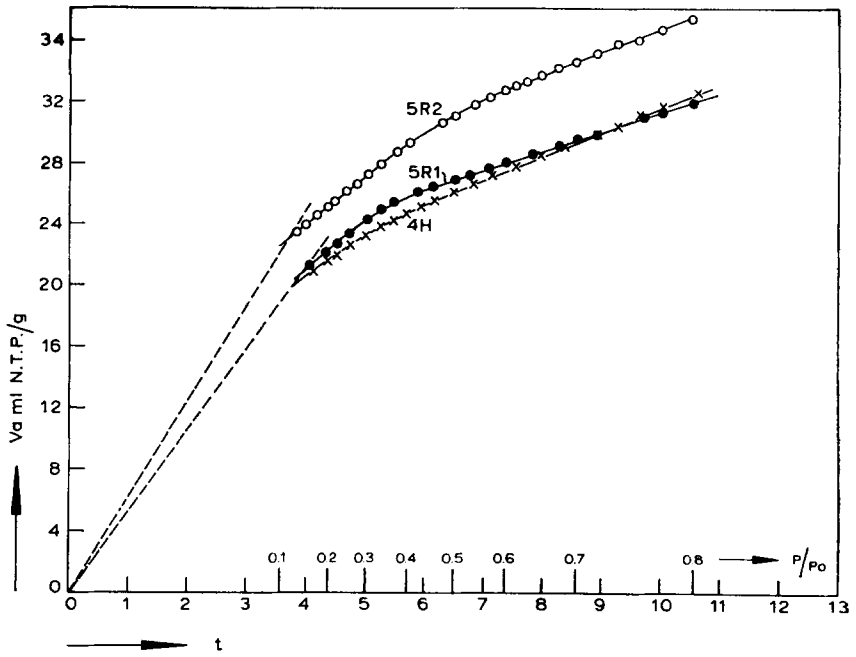

FIG. 3. t Plots of the adsorption branch of nitrogen isotherms on various graphitic oxides (*17*).

suitable for testing the present method of calculation. t Plots of the boehmite samples of Lippens (*20*), furnishing us with the surface area present in wide pores, have been published before. t Plots of the samples of van Doorn are represented in Fig. 3 and indicate the presence of a substantial amount of submicropores. In Table 2, the cumulative surface areas at the closing point of the hysteresis loop are presented together with the cumulative surface areas as calculated with the aid of the uncorrected Kelvin equation (8), and the areas present in wide pores, as determined from the t plots. Agreement between the results of the present treatment and the t area (with which we mean the surface area deduced from the slope of the t plot) in wide pores is especially satisfactory for the graphitic oxide samples. For the samples BoG 450 and BoG 580, where a large amount of surface area was still present

TABLE 2

CUMULATIVE SURFACE AREAS AND PORE VOLUMES IN SLIT-SHAPED PORES, CALCULATED FROM THE DESORPTION BRANCH OF NITROGEN SORPTION ISOTHERMS BY MEANS OF A CORRECTED KELVIN EQUATION, AS COMPARED TO THE RESULTS OF A CLASSICAL PORE DISTRIBUTION CALCULATION

Sample code[a]	p/p_0 of closing point of hysteresis loop	S_t (m^2/g)	S_{cum} (m^2/g)	$S_{cum\ class}$ (m^2/g)	V_p (ml/g)	V_{cum} (ml/g)	$V_{cum\ class}$ (ml/g)
BoG 450	0.46	5.1	8.5	11.7	0.039	0.043	0.045
BoG 580	0.44	17.2	21.5	30.0	0.085	0.089	0.093
BoG 750	0.48	19.1	16.2	22.0	0.139	0.138	0.142
Graph-ox. 4H	0.45	22.2	21.8	30.9	0.073	0.077	0.082
Graph-ox. 5RI	0.47	19.5	21.2	30.5	0.071	0.072	0.078
Graph-ox. 5RII	0.41	23.5	20.1	28.2	0.069	0.069	0.073

[a] The BoG samples were taken from the publication of Lippens (*16*). The graphitic oxide sample results were published by van Doorn (*17*).

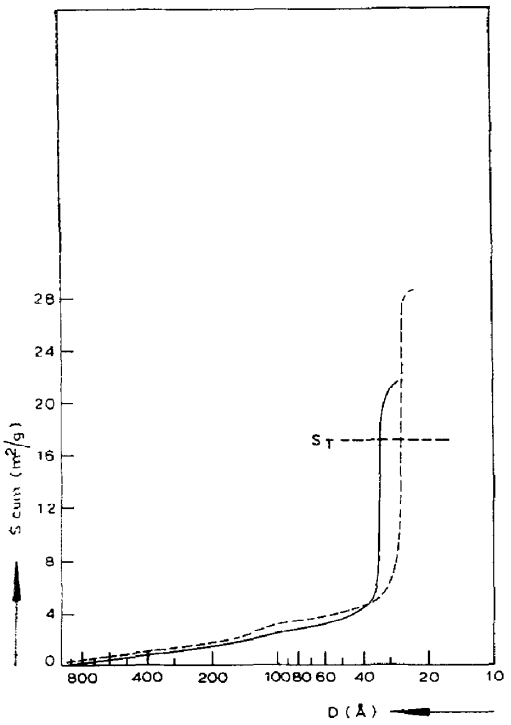

FIG. 4a

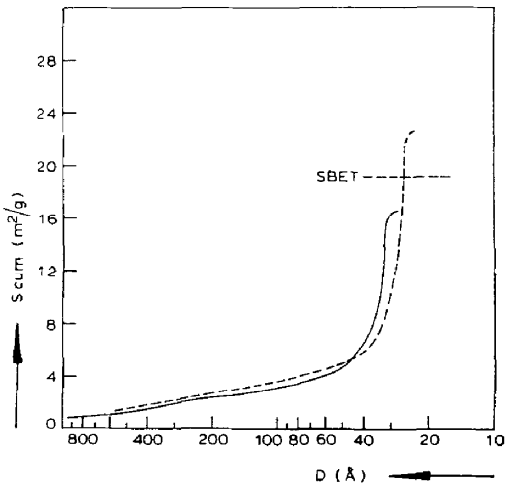

FIG. 4b

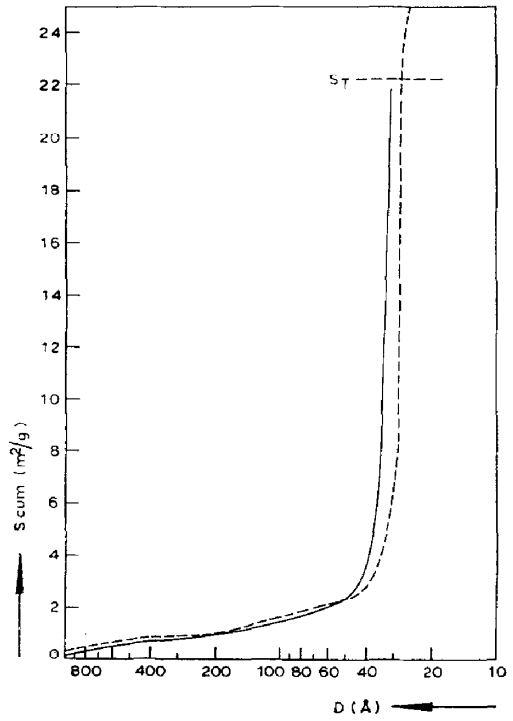

FIG. 4c

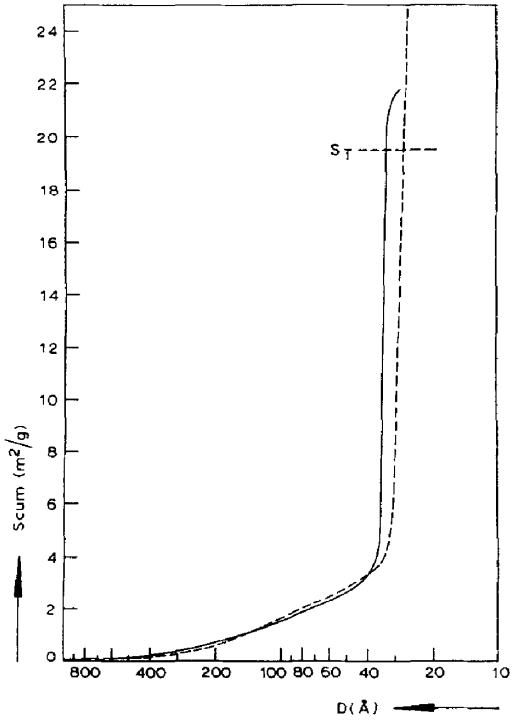

FIG. 4d

FIG. 4. Cumulative surface area distribution curves. Solid lines: calculated with the aid of the uncorrected Kelvin equation. Sample BoG 580 [Lippens (*16*)]. Sample BoG 750 [Lippens (*16*)]. Sample graphitic oxide 4H [van Doorn (*17*)]. Sample graphitic oxide 5RI [van Doorn (*17*)].

in submicropores, the agreement is less satisfactory. The results from the use of the uncorrected Kelvin equation in all cases are high in comparison to the t area present in wide pores.

In general, if the cumulative surface area at the closing point of the hysteresis loop is far higher than the appropriate t area, this may be an indication of wide-bodied ink bottles, exhibiting a B-type hysteresis loop and no upward deviations in the t plot, these latter deviations occurring at too high a relative pressure. Small deviations between S_t and S_{cum}, however, may be caused by the approximate character of any pore model idealization as well as by uncertainties in the determination of surface areas from sorption data (*21*). Their importance must not be overstressed.

In Fig. 4, for some samples the cumulative surface area distribution functions as calculated with the aid of (9) and with the uncorrected Kelvin equation, respectively, are shown. The shift to larger pore width of the distribution function by application of the proper corrections for the influence of sorption, is clearly demonstrated.

References

1. Broekhoff, J. C. P., and de Boer, J. H., *J. Catalysis* **9**, 8 (1967).
2. Broekhoff, J. C. P., and de Boer, J. H., *J. Catalysis* **9**, 15 (1967).
3. Broekhoff, J. C. P., and de Boer, J. H., *J. Catalysis* **10**, 153 (1968).
4. Broekhoff, J. C. P., and de Boer, J. H., *J. Catalysis* **10**, 366 (1968).
5. Broekhoff, J. C. P., and de Boer, J. H., *J. Catalysis* **10**, 375 (1968).
6. Derjaguin, B. V., *Proc. Intern. Congr. Surface Activity, 2nd, London, 1957* **2**, 153 (Butterworth, London, 1957).
7. de Boer, J. H., Linsen, B. G., and Osinga, Th. J., *J. Catalysis* **4**, 643 (1965).
8. de Boer, J. H., Linsen, B. G., and Heuvel, A. v. d., *J. Catalysis* **3**, 268 (1964).
9. Kiselev, A. V., *Proc. Intern. Congr. Surface Activity, 2nd, London, 1957* **2**, 168 (Butterworth, London, 1957).
10. Brunauer, S., Mikhail, R. Sh., and Bodor, E. E., *J. Colloid Interface Sci.* **24**, 451 (1967).
11. Adam, N. K., "The Physics and Chemistry of Surfaces," p. 13. Oxford Univ. Press, London and New York, 1930.
12. Adamson, A. W., and Ling, I., *Advan. Chem.* **43**, 57 (1964).
13. Gibbs, J. W., "Collected Papers," Vol. I, p. 230. Dover, New York, 1961.
14. Steggerda, J. J., Thesis, Delft, The Netherlands, p. 93 (1955).
15. Innes, W. B., *Anal. Chem.* **29**, 1069 (1957).
16. de Boer, J. H., Linsen, B. G., Plas, Th. v. d., and Zondervan, G. J., *J. Catalysis* **4**, 649 (1965).
17. de Boer, J. H., Lippens, B. C., Linsen, B. G., Broekhoff, J. C. P., van den Heuvel, A., and Osinga, Th. J., *J. Colloid Interface Sci.* **21**, 405 (1966).
18. de Boer, J. H., and Lippens, B. C., *J. Catalysis* **3**, 38 (1964).
19. van Doorn, A. B. C., Thesis, Delft, The Netherlands, pp. 63, 65 (1957).
20. Lippens, B. C., and de Boer, J. H., *J. Catalysis* **4**, 319 (1965).
21. de Boer, J. H., and Broekhoff, J. C. P., *Proc. Koninkl. Ned. Akad. Wetenschap.* **B70**, 342 (1967).